Accuracy of Temporo-Spatial and Lower Limb Joint Kinematics Parameters Using OpenPose for Various Gait Patterns With Orthosis

Masataka Yamamoto, *Member, IEEE*, Koji Shimatani, Masaki Hasegawa, Yuichi Kurita, *Member, IEEE*, Yuto Ishige, and Hiroshi Takemura, *Member, IEEE*

***Abstract*— A cost-effective gait analysis system without attachments and specialized large environments can provide useful information to determine effective treatment in clinical sites. This study investigates the capability of a single camera-based pose estimation system using OpenPose (OP) to measure the temporo-spatial and joint kinematics parameters during gait with orthosis. Eleven healthy adult males walked under different conditions of speed and foot progression angle (FPA). Temporo-spatial and joint kinematics parameters were measured using a single camera-based system with OP and a three-dimensional motion capture system. The limit of agreement, mean absolute error, absolute agreement ($ICC_{2,1}$), and relative consistency ($ICC_{3,1}$) between the systems under each condition were assessed for reliability and validity. The results demonstrated that most of the ICC for temporo-spatial parameters and hip and knee kinematics parameters were good to excellent (0.60 - 0.98). Conversely, most of the ICC for ankle kinematics in all conditions were poor to fair (<0.60). Thus, the gait analysis using OP can be used as a clinical assessment tool for determining the temporo-spatial, hip, and knee sagittal plane angles during gait.**

***Index Terms*— Human pose estimation, gait analysis, kinematics, biomechanics, orthosis.**

Manuscript received March 22, 2021; revised August 6, 2021 and November 6, 2021; accepted December 10, 2021. Date of publication December 16, 2021; date of current version December 24, 2021. This work was supported in part by the Japan Society for the Promotion of Science (JSPS) KAKENHI under Grant JP19K20748. *(Corresponding author: Masataka Yamamoto.)*

This work involved human subjects or animals in its research. Approval of all ethical and experimental procedures and protocols was granted by the Ethics Committee of the Faculty of Health and Welfare at the Prefectural University of Hiroshima under Application No. 15MH036, and performed in line with the Declaration of Helsinki.

Masataka Yamamoto is with the Department of Mechanical Engineering, Tokyo University of Science, Noda 278-8510, Japan, and also with the Graduate School of Advanced Science and Engineering, Hiroshima University, Higashi-Hiroshima 739-8527, Japan (e-mail: m-yamamoto@rs.tus.ac.jp).

Koji Shimatani and Masaki Hasegawa are with the Faculty of Health and Welfare, Prefectural University of Hiroshima, Mihara 723-0053, Japan (e-mail: shimatani@pu-hiroshima.ac.jp; m-hasegawa@pu-hiroshima.ac.jp).

Yuichi Kurita is with the Graduate School of Advanced Science and Engineering, Hiroshima University, Higashi-Hiroshima 739-8527, Japan (e-mail: ykurita@hiroshima-u.ac.jp).

Yuto Ishige and Hiroshi Takemura are with the Department of Mechanical Engineering, Tokyo University of Science, Noda 278-8510, Japan (e-mail: 7517004@ed.tus.ac.jp; takemura@rs.tus.ac.jp).

Digital Object Identifier 10.1109/TNSRE.2021.3135879

I. Introduction

GAIT analysis is a crucial assessment for gait disorders in clinical site. Gait parameters, such as temporo-spatial and kinematics data obtained from gait analysis systems, can provide useful information to determine the effectiveness of rehabilitation and understand the gait mechanism. In particular, sagittal plane joint angles were commonly used as important kinematics variables in gait analysis. Temporo-spatial and kinematics variables have been used for predicting fall risk in elderly people [1] and assessing the treatment effect of rehabilitation for neurological disorders [2], [3]. The three-dimensional motion capture system (3DMC) is a typical tool for gait assessment that can accurately measure these gait parameters. Optoelectronic 3DMC system has reliability and repeatability of gait parameters and kinematics [4], [5]. Although 3DMC is the gold standard in gait assessment, it is difficult to use in clinical settings, as it requires specialized environments, many devices, technical skills, and considerable cost [6]. As an alternative, a depth camera-based markerless human pose estimation system can be used for gait measurement in clinical sites. For example, a Microsoft Kinect sensor, which predicts human movement and pose through a depth camera, has been used for healthcare and body movement estimation. This sensor can measure temporo-spatial parameters from human gait and can thus be used as a gait assessment tool [7]. According to previous studies, the Kinect can measure temporo-spatial parameters, such as gait speed, step time, and step length, with high reliability [8], [9]. It can also be used as an exergaming aid for the prefrail and frail elderly and in the assessment of the cognitive function by measuring dual-task gait, as it can accurately estimate human poses based on a machine learning algorithm [10], [11]. However, the measurement of lower extremity sagittal plane kinematics using a depth camera-based estimation system is not highly accurate. In addition, depth cameras cannot easily measure fast joint movement because of a limitation of sampling rate. Sampling rate of depth camera system for motion capture was 30 Hz, while 3DMC for gait analysis was more than 60 or 100Hz [7]. Lower sampling rate might loss important kinematic data such as rapid ankle movement in early and late stance phase.

Recently, red, green, and blue (RGB) camera-based two-dimensional (2D) markerless systems, such as PoseNet [12] and OpenPose (OP) [13], have been developed for estimating human poses and body segment tracking. Although these systems do not use depth sensors, it can estimate the

human-body joint center point with 2D images or videos using convolutional neural networks (CNNs). OP is used for development of automated Parkinson's disease motor assessment tool [14]. OP might be used as an alternative to 3DMC for kinematics analysis at a clinical site. However, only a few studies have been conducted on the estimation accuracy of kinematics parameters of human gait. Although hip and knee joint angles in the sagittal plane were compared between OP and Inertial Measurement Units, these angles have only been evaluated under comfortable gait condition and the results showed insufficient accuracy [15]. Moreover, it is important to estimate gait while wearing assist devices, because many patients use an orthosis for treatment, but the estimation accuracy of gait kinematics with orthosis is still not clear. Ankle–foot orthosis (AFO) is mainly used for gait rehabilitation of neurological disorders, and can improve gait speed, gait kinematics, and abnormal gait patterns [16]–[18]. The lower extremity joint angles during gait with orthosis can be objectively assessed using an RGB camera-based pose estimation system without a specialized environment; this can contribute to an efficient design of the treatment methods. Therefore, this study aims to evaluate the accuracy of OP in estimating temporo-spatial and lower extremity joint angles during gait with orthosis. In addition, we measure various gait speed and foot progression angle (FPA) conditions, assuming that they are often observed in clinical sites. We hypothesize that this system has high agreement and consistency with 3DMC; however, the ankle angle in large FPA condition has a large error between OP and 3DMC.

II. Methods

A. Participants

Eleven healthy adult males (mean ± standard deviation, age: 23.2 ± 1.4 years, height: 1.73 ± 0.05 m, mass: 61.2 ± 9.7 kg) participated in this study. The following exclusion criteria were used: < 20 years of age; limitation of physical activity due to current injury or disease; history of lower limb surgery, neurological disorders, or cardiac disease; and pain during gait. All procedures were approved by the ethics committee of the Faculty of Health and Welfare at the Prefectural University of Hiroshima (15MH036), and written informed consent was obtained from all participants. This study was performed in accordance with the Declaration of Helsinki.

B. Experimental Setup and Procedures

The articulated AFO was used for evaluating the reliability of the pose estimation system during gait with orthosis in this study. The participants wore the AFO on their right foot and the same type of size-matched shoe on their left foot. Although they used the AFO, its springs, which generated stiffness, were removed because we wanted to exclude the effect of stiffness on gait. This AFO exhibited dorsiflexion and plantarflexion movement without resistance. Seven infrared cameras OptiTrack motion capture system (NaturalPoint, Corvallis, OR, USA) and Skycom software (Accuity, Tokyo, Japan) were used for measurement of 3DMC. In total, 31 reflective markers were placed on the anatomical landmarks. For estimating by OP, an acA720-290gc camera with pixel resolution

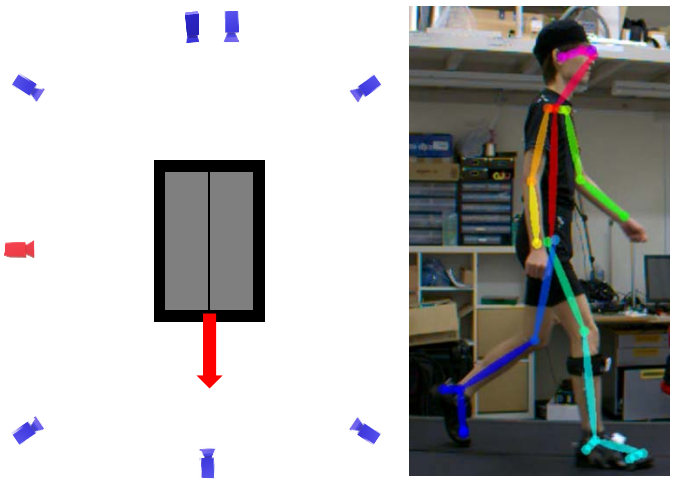

Fig. 1. Experimental setup and body model of OP (BODY_25) used in this study. The left figure shows overhead view of the experimental setup. The red arrow indicates gait direction. The approximate position of the 2D video camera (red) and infrared cameras for 3DMC (blue) are also indicated. The right figure shows keypoints estimated by OP.

of 720 × 520 (Basler AG, Ahrensburg, Germany) was positioned on the right side of the measurement area to capture a 2D video of walking on a treadmill (Bertec Corporation, Columbus, OH, USA). The camera was placed 3 m away from participants, and its height was set at each participant's greater trochanter. The experimental setup and keypoints of OP were shown in Fig. 1. The sampling rate of both 3DMC and video data was 100 Hz.

OP, an open source human pose estimation system, was used to estimate the temporo-spatial and kinematics parameters during gait. Using two branch multistage convolution neural network (CNN), the OP estimated the joint locations from each RGB image as input. In the first stage, the part affinity fields, which form a set of 2D vector fields that encode the location and orientation of extremities over the RGB images, were predicted [13]. In the second stage, the confidence maps of each body segment's location were predicted. Finally, both stages were parsed to output the 2D keypoints of people in the images. More details of OP can be found in a previous study [13]. The 2D coordinates of 25 body keypoints in each video frame captured by the OP were used for the analysis (Fig. 1).

The participants were asked to walk under four conditions on a treadmill: self-selected comfortable speed with normal and large FPA conditions, and slow speed with normal and large FPA conditions. The order of four gait conditions was randomized in each participant. The slow speed was set to 0.60 m/s, which indicated the gait speed of the average limited community ambulation in individuals after a stroke [19], [20]. Before the experimental measurements, the participants walked on a 15 m walkway under the ground condition at their self-selected speed. Thereafter, these gait speeds were used for experimental measurement with the treadmill under the self-selected speed conditions by referring to a previous study [21]. In normal FPA conditions, they were asked to walk as usual. In large FPA conditions, the FPA was set at 50° by a physical therapist, and it was also

checked during gait by 3DMC. Considering large FPA is very important because FPA increases during pathological gait, such as stroke and knee osteoarthritis [22]–[24]. In addition, it is also important for 2D video analysis to investigate accuracy in large FPA condition including out of 2D image plane excessive motion. Although the self-selected speed with large FPA condition might be not observed in clinical site, we added this to evaluate whether the OP could measure such as high difficulty condition. Before the measurement, the participants were allowed to practice sufficient walking under each condition. After sufficient gait practice, the gait trials were measured at 15 s intervals.

C. Data Analysis and Statistical Analysis

Temporo-spatial parameters obtained from 3DMC methods were used as the gold standard; gait speed, stride, stride time, and step length were used as this parameters. The midpoint of both posterior superior iliac spine (PSIS) markers was used to calculate the gait speed in 3DMC. In OP, the gait speed was calculated using the mean midhip keypoint velocity in the sagittal plane from the video data. We also defined the initial contact and toe-off times from the 3DMC and OP data by referring to a previous study [25]. The initial contact was defined as the maximum point of antero-posterior distance between the heel and midpoint of PSIS in 3DMC or the midhip in OP, whereas toe off was defined as the minimum point of antero-posterior distance between the heel and midpoint of the PSIS or midhip. The gait trials were conducted using a treadmill; the stride was calculated as

$$stride = V_{tr}T + (Xheel_{i+1} - Xheel_i) \tag{1}$$

where V_{tr} indicates the treadmill belt speed and T indicates the stride time based on the defined initial contact time. *Xheel* is the heel keypoint and marker coordinates of the sagittal plane (X) on the i and $i+1$th initial contacts, respectively. In addition, we calculated the representative kinematics parameters of the hip, knee, and ankle angles for gait assessment from the 3DMC and OP data by referring to previous studies [26]–[28]. 3DMC joint angles were calculated in a joint specific sagittal plane. The hip, knee, and ankle angles in the sagittal plane of OP were calculated as follows:

$$angle = \cos^{-1}\frac{\vec{S}_p \cdot \vec{S}_d}{\left|\vec{S}_p\right|\left|\vec{S}_d\right|} \tag{2}$$

where $\vec{S}_p$ and $\vec{S}_d$ are the proximal and distal body segment vectors, respectively, used to calculate the coordinates of the related keypoints. In one example, the right knee's flexion–extension angle was calculated from the right thigh's and right lower leg's segment vectors. The right thigh's segment vector was calculated from the coordinates of the right hip and knee keypoints. The right lower leg's segment vector was calculated from the coordinates of the right knee and ankle keypoints. We also compared the trailing limb angles (TLA) obtained from the 3DMC and OP methods. Previous studies have reported the TLA related forward propulsive force and gait speed in subjects with stroke [27], [29], [30]. In the 3DMC method, TLA is defined as the angle between a vector joining the greater trochanter with the fifth metatarsal head and the laboratory's vertical axis [30]. By contrast, in the OP method, TLA is defined as the angle between a vector joining the right hip and the small toe of the keypoint and the laboratory's vertical axis. In the stance phase, the peak hip flexion, hip extension, TLA, knee flexion, dorsiflexion, and plantarflexion values obtained using the 3DMC and OP methods were compared. As an index of knee flexion in the stance phase, the knee flexion angle in the initial contact and peak knee flexion angle from the initial contact to the midstance (early stance) were measured. In addition, we compared the peak knee flexion angles during the swing phase obtained using the two methods.

All statistical analyses were performed using the R version 3.6.3 software (CRAN, freeware). For each parameter, the assumption of normality was assessed by Shapiro-Wilk test. The Bland–Altman method was used to assess the limit of agreement (LOA) and relative LOA (LOA%) between the data of the 3DMC and OP methods [31]. Bland-Altman method checks for the systematic bias in the measurement values. The 95% LOA was calculated as 1.96 times the standard deviation (SD) of the difference between the 3DMC and OP methods. If the LOA range was narrow, the two methods could be used interchangeably. LOA% represents the absolute difference between the 3DMC and OP methods as a percentage of measured data. The mean absolute error (MAE) of the temporo-spatial parameter and joint kinematics data between both methods was also calculated for each condition. This error was the absolute value of the difference between both systems, then averaged across each participant. In addition, a one-way repeated measures analysis of variance was used to compare the MAEs of temporo-spatial and kinematics parameters among the four conditions, followed by Shaffer's modified sequentially rejective Bonferroni procedure as a post hoc test. The Friedman test was used to compare the data without normality among the four conditions. Furthermore, the interclass correlation coefficient (ICC) was calculated to determine absolute agreement ($ICC_{2,1}$) and relative consistency ($ICC_{3,1}$) between the gait and kinematic parameters from both systems. The ICC values were interpreted as poor (< 0.40), fair (0.40 - < 0.60), good (0.60 - < 0.75), and excellent (≥ 0.75) [32]. Finally, the cross-correlation coefficients (CCC) between both systems were used to evaluate the similarity of angles during gait cycle. The CCC values were interpreted as weak or no coupling ($-0.3 < CCC < 0.3$), moderate coupling ($0.3 \leq CCC < 0.70$ or $-0.7 < CCC \leq -0.3$), and strong coupling ($CCC > 0.7$ or $CCC < -0.7$) [33]. The statistical significance was set at $p < 0.05$.

III. Results

The LOA values obtained under each condition are listed in Table I. The mean, SD, MAE, and $ICC_{2,1}$ and $ICC_{3,1}$ values of the temporo-spatial parameters and kinematics parameters at the self-selected gait speed and slow speed are listed in Tables II and III, respectively. The LOA of these parameters were almost similar under each condition except for peak knee

TABLE I
LOA OF TEMPORO-SPATIAL AND KINEMATICS PARAMETERS IN THE FOUR CONDITIONS

		self-selected		slow	
		LOA (lower, upper)	LOA% (lower, upper)	LOA (lower, upper)	LOA% (lower, upper)
Gait speed (m/s)	normal	0.01 (-0.01, 0.03)	0.55 (-0.67, 1.78)	-0.01 (-0.01, 0.01)	-1.07 (-3.31, 1.17)
	large FPA	0.01 (-0.02, 0.03)	0.28 (-1.62, 2.18)	0.01 (-0.01, 0.01)	0.36 (-1.37, 2.09)
Stride (m)	normal	-0.02 (-0.05, 0.01)	-1.43 (-3.11, 0.26)	0.01 (-0.03, 0.03)	0.51 (-2.90, 3.93)
	large FPA	-0.01 (-0.06, 0.03)	-0.96 (-3.93, 2.00)	0.01 (-0.03, 0.03)	0.11 (-3.21, 3.44)
Stride time (s)	normal	0.01 (-0.01, 0.01)	0.08 (-0.91, 1.09)	-0.01 (-0.03, 0.02)	-0.01 (-1.71, 1.70)
	large FPA	-0.01 (-0.02, 0.01)	-0.62 (-2.37, 1.13)	0.02 (-0.01, 0.05)	1.24 (-0.94, 3.42)
Step length (m)	normal	0.01 (-0.04, 0.05)	1.12 (-4.19, 6.44)	-0.01 (-0.04, 0.03)	-0.75 (-9.04, 7.55)
	large FPA	0.02 (-0.02, 0.05)	3.51 (-2.82, 9.83)	0.03 (0.01, 0.06)	10.83 (-0.70, 22.37)
Peak hip flexion-stance (deg)	normal	-3.11 (-5.69, -0.53)	-12.92 (-23.07, -2.78)	0.09 (-2.11, 2.29)	-0.15 (-9.58, 9.27)
	large FPA	-4.65 (-8.12, -1.18)	-18.27 (-32.06, -4.48)	-1.60 (-4.97, 1.76)	-9.04 (-25.64, 7.57)
Peak hip extension-stance (deg)	normal	-2.58 (-6.35, 1.19)	18.84 (-3.55, 41.22)	3.59 (-0.19, 7.37)	-28.50 (-58.32, 1.33)
	large FPA	0.33 (-4.52, 5.19)	-0.95 (-34.29, 32.39)	2.17 (-1.37, 5.71)	-15.30 (-44.89, 14.29)
TLA (deg)	normal	1.30 (0.51, 2.09)	4.89 (1.71, 8.06)	1.32 (0.11, 2.53)	8.05 (-0.02, 16.12)
	large FPA	3.04 (1.80, 4.28)	11.73 (6.47, 17.00)	-0.83 (-2.15, 0.49)	-6.03 (-15.57, 3.51)
Peak knee flexion-initial contact (deg)	normal	3.61 (1.52, 5.70)	103.02 (42.63, 163.42)	2.71 (0.02, 5.39)	43.92 (7.75, 80.09)
	large FPA	1.79 (-0.90, 4.48)	17.39 (-5.51, 40.28)	3.31 (0.03, 6.59)	42.26 (-0.27, 84.78)
Peak knee flexion-early stance (deg)	normal	2.47 (0.57, 4.38)	8.46 (1.92, 15.00)	1.56 (-1.77, 4.90)	9.42 (-10.40, 29.23)
	large FPA	5.18 (1.97, 8.38)	18.39 (7.28, 29.50)	2.26 (-0.37, 4.89)	9.65 (-4.80, 24.11)
Peak knee flexion-swing (deg)	normal	1.95 (0.32, 3.58)	2.60 (0.44, 4.77)	1.92 (-0.22, 4.06)	2.90 (-0.44, 6.25)
	large FPA	7.51 (4.06, 10.96)	12.50 (6.22, 18.79)	5.39 (-0.48, 11.26)	13.18 (-1.19, 27.54)
Peak dorsiflexion-stance (deg)	normal	4.42 (-1.23, 10.09)	28.74 (-6.06, 63.54)	5.79 (2.40, 9.17)	44.30 (13.07, 75.53)
	large FPA	2.29 (-6.66, 11.24)	-97.71 (-498.41, 303.00)	2.46 (-4.17, 9.08)	44.22 (-41.79, 130.23)
Peak plantarflexion-stance (deg)	normal	7.11 (2.72, 11.50)	-52.45 (-84.08, -20.82)	7.55 (3.79, 11.31)	-79.04 (-119.83, -38.24)
	large FPA	12.20 (2.63, 21.78)	-81.24 (-150.75, -11.73)	12.13 (4.50, 19.76)	-109.16 (-181.93, -36.39)

Data are presented as the mean, lower, and upper values.

flexion during swing phase and peak plantarflexion during stance phase.

A. Temporo-Spatial Parameters

The ICC of temporo-spatial parameters in each condition was almost excellent. In addition, no statistically significant difference was found in the MAEs of gait speed, stride, and step length among the four conditions ($p = 0.06$, $p = 0.61$, and $p = 0.99$, respectively); however, the stride time was significantly different ($p = 0.04$). Nevertheless, multiple comparison analyses did not vary significantly among the four conditions, and the lowest p value was 0.10, comparing slow speed with normal task and self-selected speed with normal task.

B. Kinematics Parameters

The hip, knee, and ankle angles during the gait cycle in each condition are shown in Figure 2, 3, and 4. To summarize the results of kinematics parameters, most of the ICC for hip and knee angles in each condition were good to excellent. However, most of the ICC for ankle angles were poor. CCC of hip, knee, ankle joint angle in each condition were strong coupling except for ankle angle in slow speed with large FPA condition.

The MAE of the peak hip flexion angle in the stance phase significantly differed among the four conditions ($p = 0.04$). Nevertheless, multiple comparison analyses did not vary significantly among these conditions, and the lowest p value was 0.18, comparing slow speed with normal task and slow speed with large FPA. No statistically significant

TABLE II
TEMPORO-SPATIAL AND KINEMATICS PARAMETERS OF BOTH SYSTEMS IN SELF-SELECTED SPEED CONDITIONS

		OP (mean ± SD)	3DMC (mean ± SD)	MAE (mean ± SD)	ICC (2,1) (95% CI)	ICC (3,1) (95% CI)
Gait speed (m/s)	normal	1.39 ± 0.17	1.38 ± 0.16	0.01 ± 0.02	0.98 (0.96, 0.99)	0.98 (0.96, 0.99)
	large FPA	1.39 ± 0.17	1.37 ± 0.17	0.02 ± 0.03	0.98 (0.93, 0.99)	0.98 (0.93, 0.99)
Stride (m)	normal	1.46 ± 0.15	1.46 ± 0.19	0.03 ± 0.03	0.98 (0.91, 0.99)	0.98 (0.95, 0.99)
	large FPA	1.38 ± 0.22	1.38 ± 0.21	0.04 ± 0.04	0.96 (0.88, 0.99)	0.96 (0.87, 0.99)
Stride time (s)	normal	1.06 ± 0.06	1.06 ± 0.07	0.01 ± 0.01	0.98 (0.93, 0.99)	0.98 (0.93, 0.99)
	large FPA	1.00 ± 0.04	1.00 ± 0.04	0.02 ± 0.01	0.88 (0.62, 0.96)	0.87 (0.60, 0.96)
Step length (m)	normal	0.73 ± 0.11	0.74 ± 0.10	0.04 ± 0.03	0.89 (0.64, 0.97)	0.88 (0.62, 0.97)
	large FPA	0.69 ± 0.14	0.70 ± 0.12	0.04 ± 0.03	0.94 (0.79, 0.98)	0.94 (0.80, 0.98)
Peak hip flexion-stance (deg)	normal	30.16 ± 6.79	27.05± 8.63	3.91 ± 2.06	0.85 (0.27, 0.96)	0.91 (0.71, 0.98)
	large FPA	32.08 ± 7.56	27.43 ± 9.52	5.13 ± 3.72	0.77 (0.07, 0.94)	0.87 (0.59, 0.96)
Peak hip extension-stance (deg)	normal	15.94 ± 5.52	18.52 ± 2.60	4.47 ± 2.79	0.35 (-0.17, 0.76)	0.40 (-0.23, 0.79)
	large FPA	14.38 ± 5.09	14.05 ± 4.25	3.86 ± 4.58	0.17 (-0.53, 0.69)	0.15 (-0.46, 0.67)
TLA (deg)	normal	28.31 ± 3.84	26.86 ± 4.13	1.30 ± 1.10*	0.92 (0.29, 0.98)	0.96 (0.86, 0.99)
	large FPA	28.44 ± 4.60	25.22 ± 4.72	3.04 ± 1.72	0.78 (-0.07, 0.96)	0.93 (0.76, 0.98)
Peak knee flexion-initial contact (deg)	normal	2.67 ± 3.24	6.28 ± 3.13	3.66 ± 2.55	0.41 (-0.12, 0.80)	0.66 (0.13 0.90)
	large FPA	11.37 ± 5.68	13.16 ± 5.21	2.67 ± 2.67	0.78 (0.38, 0.94)	0.81 (0.43, 0.94)
Peak knee flexion-early stance (deg)	normal	27.17 ± 6.07	29.64 ± 6.93	3.09 ± 1.39	0.87 (0.27, 0.97)	0.93 (0.77, 0.98)
	large FPA	25.90 ± 7.75	31.07 ± 9.03	5.29 ± 3.86	0.75 (-0.03, 0.94)	0.89 (0.63, 0.97)
Peak knee flexion-swing (deg)	normal	73.84 ± 3.10	75.79 ± 3.19	2.17 ± 1.79* †	0.67 (0.03, 0.91)	0.78 (0.38, 0.94)
	large FPA	59.34 ± 8.47	66.85 ± 5.66	7.51 ± 4.33	0.54 (-0.10, 0.87)	0.82 (0.46, 0.95)
Peak dorsiflexion-stance (deg)	normal	15.20 ± 5.52	19.62 ± 4.54	6.87 ± 4.50	0.01 (-0.39, 0.52)	0.01 (-0.57, 0.58)
	large FPA	11.84 ± 8.60	14.13 ± 7.78	9.90 ± 4.90	0.06 (-0.57, 0.63)	0.06 (-0.53, 0.62)
Peak plantarflexion-stance (deg)	normal	17.31 ± 7.39	10.20 ± 4.66	7.62 ± 4.69	0.37 (-0.13, 0.77)	0.60 (0.04, 0.87)
	large FPA	21.05 ± 9.15	8.85 ± 9.23	14.04 ± 9.57	0.08 (-0.19, 0.50)	0.14 (-0.47, 0.66)

* and † indicates a significant difference compared to self-selected speed with large FPA and slow speed with large FPA conditions, respectively ($p < 0.05$). ICC interpretations of excellent, good, fair, and poor were shown in blue, green, yellow, and red, respectively.

difference was found in the MAE of the hip extension angle in the initial contact among the four conditions ($p = 0.69$). In measurement of TLA, one of the participants dropped out because the greater trochanter marker could not detect sufficiently. The MAE of TLA significantly differed among the four conditions ($p = 0.02$). Multiple comparison analyses identified a significant decrease in the self-selected speed with normal task compared to self-selected speed with large FPA condition ($p = 0.02$).

In MAE of knee joint angle, no statistically significant difference was observed in the knee flexion angle in initial contact among the four conditions ($p = 0.31$). The peak knee flexion angle in the early stance phase was significantly different among the four conditions ($p = 0.04$). Nevertheless, multiple comparison analyses did not vary significantly, and the lowest p value was 0.19, comparing the self-selected speed with the normal task and that with the large FPA condition. The peak knee flexion angle in the swing phase

TABLE III
TEMPORO-SPATIAL AND KINEMATICS PARAMETERS OF BOTH SYSTEMS IN SLOW SPEED CONDITIONS

		OP (mean ± SD)	3DMC (mean ± SD)	MAE (mean ± SD)	ICC (2,1) (95% CI)	ICC (3,1) (95% CI)
Gait speed (m/s)	normal	0.61 ± 0.01	0.60 ± 0.02	0.01 ± 0.01	0.84 (0.53, 0.95)	0.84 (0.52, 0.96)
	large FPA	0.60 ± 0.01	0.60 ± 0.01	0.01 ± 0.01	0.68 (0.17, 0.90)	0.67 (0.15, 0.90)
Stride (m)	normal	0.87 ± 0.13	0.88 ± 0.11	0.03 ± 0.02	0.96 (0.87, 0.99)	0.96 (0.86, 0.99)
	large FPA	0.85 ± 0.11	0.84 ± 0.12	0.03 ± 0.02	0.95 (0.84, 0.99)	0.95 (0.82, 0.99)
Stride time (s)	normal	1.47 ± 0.16	1.48 ± 0.16	0.03 ± 0.01	0.98 (0.94, 0.99)	0.98 (0.94, 0.99)
	large FPA	1.37 ± 0.19	1.38 ± 0.19	0.06 ± 0.04	0.97 (0.90, 0.99)	0.98 (0.92, 0.99)
Step length (m)	normal	0.46 ± 0.09	0.45 ± 0.06	0.04 ± 0.02	0.83 (0.49, 0.95)	0.82 (0.46, 0.95)
	large FPA	0.37 ± 0.10	0.41 ± 0.07	0.04 ± 0.04	0.84 (0.34, 0.96)	0.90 (0.66, 0.97)
Peak hip flexion-stance (deg)	normal	20.76 ± 4.04	20.86 ± 4.94	2.15 ± 1.60	0.83 (0.47, 0.95)	0.81 (0.44, 0.95)
	large FPA	21.57 ± 4.14	19.97 ± 5.33	4.04 ± 1.64	0.60 (0.07, 0.87)	0.61 (0.05, 0.88)
Peak hip extension-stance (deg)	normal	13.10 ± 5.35	9.52 ± 2.73	4.37 ± 3.95	0.29 (-0.17, 0.71)	0.37 (-0.26, 0.78)
	large FPA	12.31 ± 4.14	10.14 ± 2.22	3.79 ± 3.03	0.09 (-0.40, 0.61)	0.11 (-0.50, 0.64)
TLA (deg)	normal	17.37 ± 4.81	16.19 ± 4.67	1.87 ± 0.93	0.91 (0.57, 0.98)	0.94 (0.78, 0.98)
	large FPA	19.25 ± 3.59	17.15 ± 3.72	2.08 ± 1.65	0.79 (0.31, 0.97)	0.83 (0.46, 0.97)
Peak knee flexion-initial contact (deg)	normal	6.00 ± 4.17	8.71 ± 3.78	3.66 ± 2.16	0.54 (-0.03, 0.85)	0.64 (0.10, 0.85)
	large FPA	12.44 ± 8.79	15.75 ± 6.95	4.34 ± 2.88	0.80 (0.28, 0.95)	0.87 (0.58, 0.96)
Peak knee flexion-early stance (deg)	normal	17.94 ± 5.82	19.51 ± 6.39	3.45 ± 2.68	0.76 (0.35, 0.93)	0.76 (0.34, 0.93)
	large FPA	20.16 ± 7.69	22.43 ± 8.32	3.09 ± 2.45	0.89 (0.56, 0.97)	0.91 (0.72, 0.98)
Peak knee flexion-swing (deg)	normal	62.05 ± 6.22	63.97 ± 7.14	2.79 ± 1.66* †	0.89 (0.55, 0.97)	0.92 (0.73, 0.98)
	large FPA	46.50 ± 11.30	51.89 ± 6.18	7.28 ± 5.30	0.59 (0.03, 0.87)	0.67 (0.16, 0.90)
Peak dorsiflexion-stance (deg)	normal	12.44 ± 5.41	18.23 ± 3.25	6.00 ± 3.91	0.30 (-0.13, 0.72)	0.55 (-0.04, 0.85)
	large FPA	10.36 ± 6.97	12.82 ± 3.38	6.97 ± 4.73	-0.15 (-0.69, 0.47)	-0.15 (-0.67, 0.46)
Peak plantarflexion-stance (deg)	normal	14.12 ± 2.89	6.56 ± 3.67	7.82 ± 4.21	-0.01 (-0.12, 0.27)	-0.02 (-0.59, 0.56)
	large FPA	17.37 ± 9.16	5.24 ± 3.92	13.43 ± 7.42	0.03 (-0.15, 0.39)	0.07 (-0.52, 0.62)

* and † indicates a significant difference compared to self-selected speed with large FPA and slow speed with large FPA conditions, respectively ($p < 0.05$). ICC interpretations of excellent, good, fair, and poor were shown in blue, green, yellow, and red, respectively.

was also significantly different among the four conditions ($p < 0.01$). The multiple comparison analyses identified a significant decrease in the slow and self-selected speeds with normal task condition compared to the self-selected speed with large FPA condition (both $p < 0.01$). In addition, the peak knee flexion angle in the swing phase was significantly decreased for the self-selected and slow speeds with normal task condition than that for a slow speed with large FPA condition (both $p = 0.03$).

Although MAE of peak dorsiflexion angle was not significantly different among the four conditions ($p = 0.10$), MAE of peak plantarflexion angle was significantly different ($p = 0.04$). However, multiple comparison analyses did not vary significantly, and the lowest p value was 0.13, comparing the slow speed with the normal task and that with the large FPA condition. Most of the $ICC_{2,1}$ and $ICC_{3,1}$ values of both parameters were poor among the four conditions

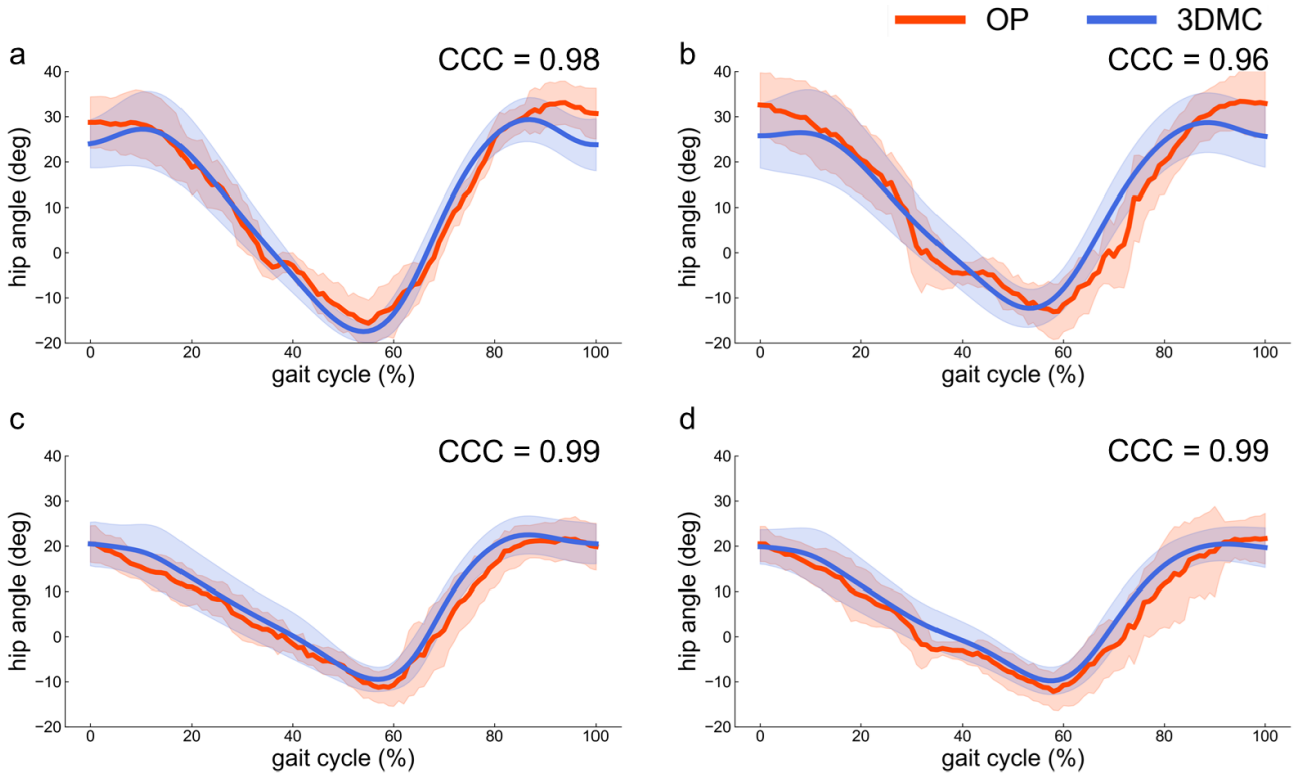

Fig. 2. Comparison between the systems of hip flexion-extension angle. Self-selected speed with normal (a) and large FPA (b) condition. Slow speed with normal (c) and large FPA (d) condition. The shade is presented as 1 SD. Flexion is defined as positive.

IV. Discussion

This study aimed to investigate the accuracy of the RGB camera-based pose estimation system to measure temporo-spatial and joint kinematics during gait with AFO. We investigated whether this system could measure the parameters under various gait conditions compared with 3DMC. The results indicated that the 2D pose estimation system using OP could measure the temporo-spatial parameters and several hip and knee joint kinematics information under various gait conditions with high agreement and consistency. Conversely, this system could not measure the ankle angle of the sagittal plane with high agreement and consistency.

The MAEs of the gait speed, stride, stride time, and step length were not statistically significant among the four conditions. A previous study conducted using a markerless pose estimation system reported that this system could measure the temporo-spatial parameters under various gait speed conditions with excellent relative association [9], [34]. We also examined large FPA conditions, where the MAE and LOA values were found to be similar among the four conditions. In addition, $ICC_{2,1}$ and $ICC_{3,1}$ of these parameters ranged from good to excellent. Although $ICC_{2,1}$ and $ICC_{3,1}$ values of the slow gait speed with large FPA condition were good, the MAE between the OP and 3DMC systems was only 0.01 m/s. This error was less than minimally clinically important difference in patients admitted to a short-term rehabilitation facility [35]. Therefore, this system can be used as an alternative to 3DMC even under slow gait speed or large FPA condition. These results were attributed to the high sampling rate and keypoint detection methods of OP. A previous study used a markerless and sensorless pose estimation system with a depth camera at a sampling rate of 30 Hz. Conversely, our study used a camera with a 100-Hz sampling rate. Moreover, the OP estimated the body keypoints using two multi-stage CNN. This combined method could improve the accuracy of keypoint detection [13]. Therefore, these results suggest that this system using OP can measure the temporo-spatial parameters under various gait conditions with high agreement and consistency of ICC.

As shown in Figures 2–4, under all conditions except the ankle joint angle, the patterns of sagittal joint angles obtained using the 3DMC and OP systems appeared to be similar. For almost all kinematics parameters of this study, an upper LOA of below 10° and a lower LOA of above –10° were obtained. This statistical decision is important; however, clinical decisions are also important for determining the amount of error that is acceptable [31]. Although it might sparsely measure the kinematics using markerless pose estimation system validation studies, we set the larger side of absolute LOA of $< 5°$ as optimal and $< 10°$ as acceptable by referring to previous studies conducted in the biomechanics field [36], [37]. For the peak hip flexion angle and TLA, the multiple comparison analyses did not vary significantly among the four conditions. In addition, the LOA of the peak hip flexion angle under all conditions ranged from acceptable to optimal. The $ICC_{2,1}$ and $ICC_{3,1}$ values of these parameters under all conditions also ranged from good to excellent. The ICC and difference between the systems were similar or more than those reported previous studies [9], [38], [39]. These results can be explained through the improved accuracy of joint location estimation by pose estimation [13]. The LOA of the peak hip extension angle

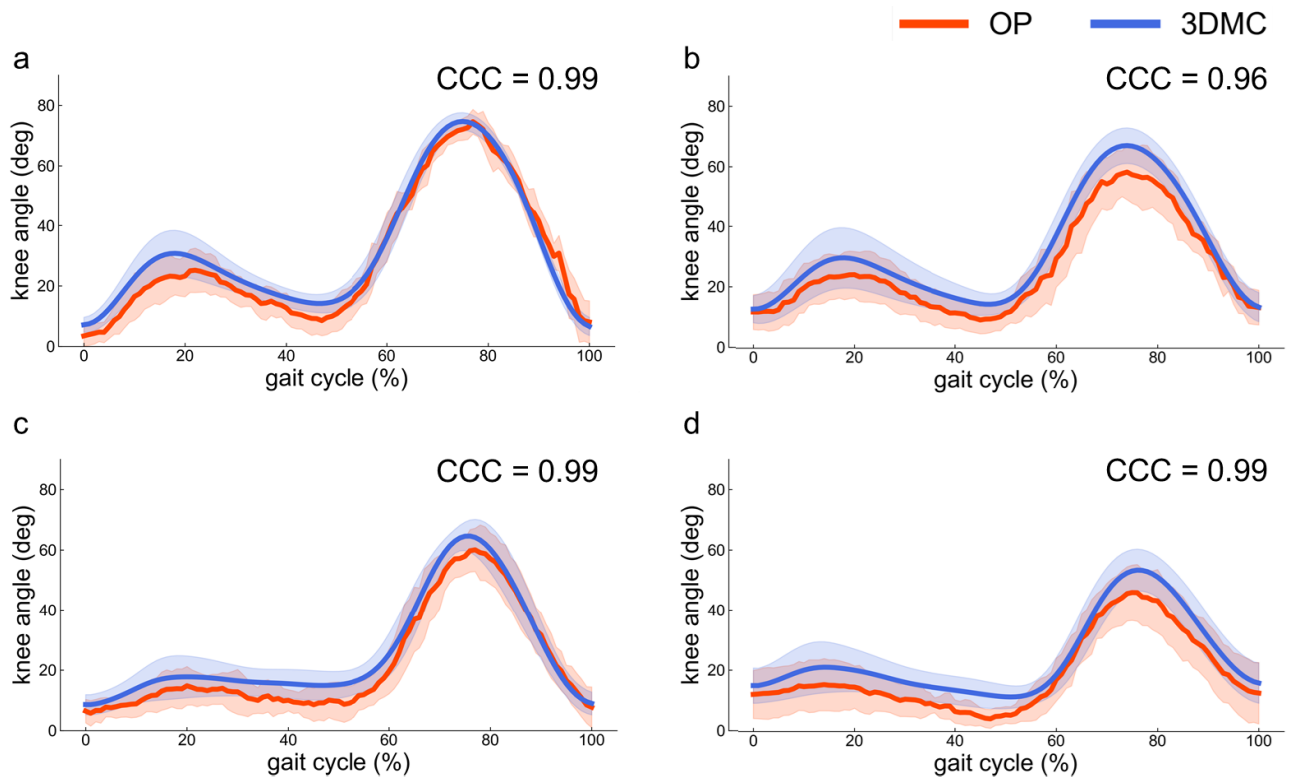

Fig. 3. Comparison between the systems of knee flexion–extension angle. Self-selected speed with normal (a) and large FPA (b) condition. Slow speed with normal (c) and large FPA (d) condition. The shade is presented as 1 SD. Flexion is defined as positive.

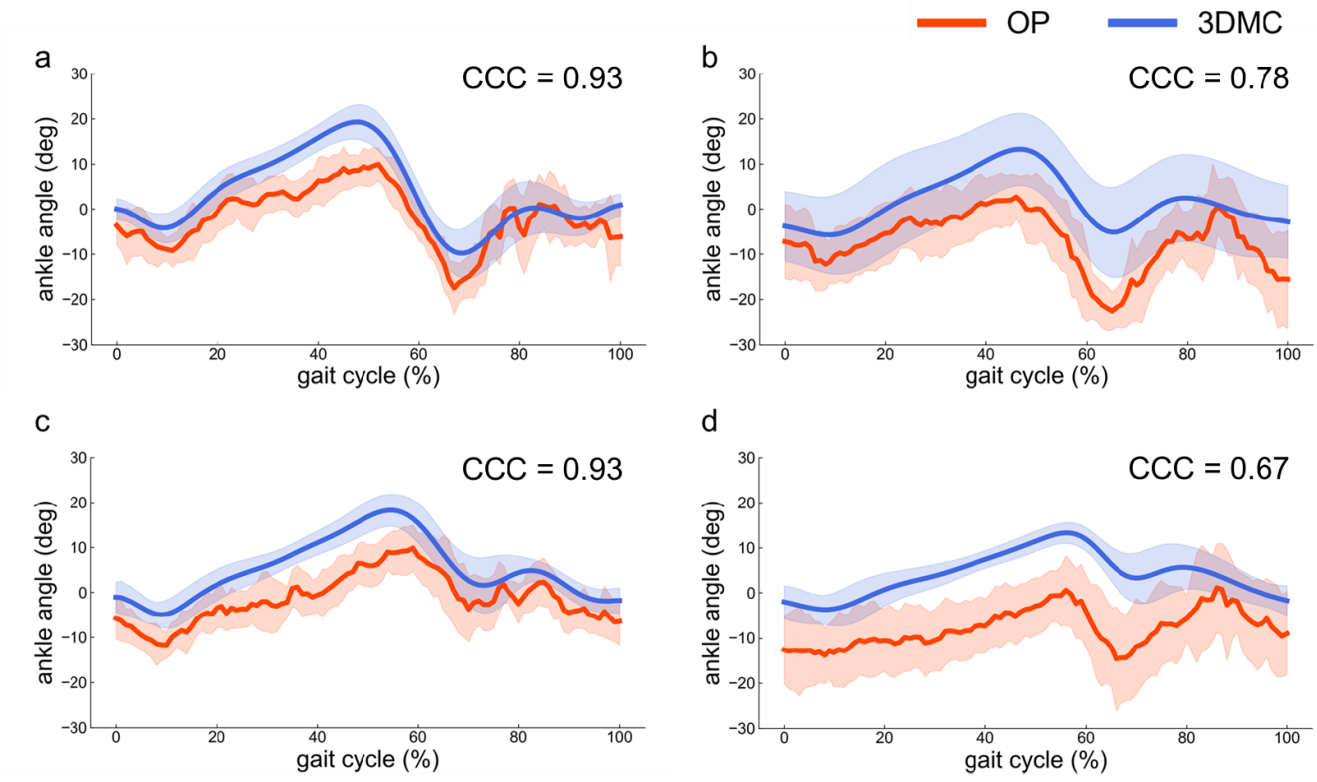

Fig. 4. Comparison between the systems of dorsiflexion–plantarflexion angle. Self-selected speed with normal (a) and large FPA (b) condition. Slow speed with normal (c) and large FPA (d) condition. The shade is presented as 1 SD. Dorsiflexion is defined as positive.

in the stance phase for all conditions ranged from acceptable to optimal. The peak hip extension angle in the stance phase did not vary significantly among the four conditions; however, $ICC_{2,1}$ and $ICC_{3,1}$ of the peak hip extension angle in the stance phase ranged from poor to fair. Although the 2D pose estimation system using OP could not obtain the peak hip extension

angle in the stance phase with high agreement and consistency of ICC, TLA might be able to provide useful hip kinematics information instead of hip extension angle. The hip extension angle in the late stance phase is noted for the lower limb posture and generates forward propulsive force; nevertheless, only focusing on a single joint might not be appropriate [40]. TLA represents the orientation of the lower limb in the late stance phase, and a previous study reported that this angle, as well as the related hip extension angle, is biomechanically important for forward propulsion [29], [30]. Therefore, the system using OP can also measure the sagittal plane of hip kinematics information with high agreement and consistency under various gait conditions.

At the knee flexion angle, the $ICC_{2,1}$ and $ICC_{3,1}$ values of the knee kinematics parameters were almost good to excellent, and their LOA values were acceptable to optimal, except for the swing phase of peak knee flexion angle in the large FPA condition. However, the $ICC_{2,1}$ of the knee flexion angle in the initial contact at both speeds under the normal condition was fair. Under both speeds with large FPA conditions, the peak knee flexion angle in the swing phase was fair. Significant difference was only found in the MAE of peak knee flexion during swing phase among the four conditions. This error might be affected because the OP might not accurately estimate joint angle in a condition such as projecting out-of-plane 3D motion due to a 2D image. Although the knee flexion angles obtained using OP in all conditions were underestimated compared to the knee flexion angle obtained using 3DMC, these trends were similar to those observed in a previous study conducted using a markerless system [39], [41]. In addition, almost all of the knee kinematics MAE were similar or less than previous studies. Xu *et al.* [39] have also reported that the Kinect-based knee joint center position was posterior to the 3DMC-based knee joint center position, and an underestimated knee flexion angle was found in the entire gait cycle under various gait speed conditions. Therefore, the results of our study might be affected by the same reason. However, the ICC and difference in knee kinematics parameters between the systems were similar or more than those reported previously [39], [41], [42]. Therefore, although the accuracy of the knee kinematics measurement was lower than that of the hip kinematics measurement in this system, the system using OP can also measure the knee kinematics information.

By contrast, the ankle kinematics parameter did not reveal measurement agreement and consistency. Although the MAEs of the peak dorsiflexion and plantarflexion angles were not statistically significant among the four conditions, the maximum MAE was $14.04 \pm 9.57°$ between the systems. In addition, the LOAs of the peak ankle angles under most of the conditions were not optimal. CCC of ankle angle in all conditions also tended to decrease compared to CCC of hip and knee joint angle. These results were similar to those obtained previously [42]. One possible reason for this is that the ankle angle velocity during gait was high and changed quickly in a short duration [43]. However, our results showed that both the ICCs of the ankle angle were poor even under the slow gait speed condition. Color problems were thought to be another possible reason for this. The 2D pose estimation using an RGB camera is influenced by the background environment. The treadmill and orthosis used in our study had similar colors. We used orthosis because we aimed to evaluate the reliability of gait assessment using a markerless pose estimation system during gait with orthosis for various gait patterns. Although we used orthosis without springs, the result of ankle angle data obtained by 3DMC was much similar to that obtained for the normal ankle angle during gait without orthosis. In addition, when we calculated the total ankle angle range in line with a previous study's outcome, the MAE of the total ankle angle ranged $5.31 \pm 4.99°$, which was lower than that observed in a previous study conducted without orthosis [42]. The shortness of the foot segment in the OP might have also affected the increase of kinematic error.

The present study has a few limitations. First, the number of participants was not very large. A small sample size may have limited the outcome from LOA and ICC, where a larger sample size could have provided better estimations. Second, the participants were only healthy adults. Future studies should investigate participants with gait disability. The accuracy of kinematic parameters in conditions including out-of-plane rotation movement should also be improved. Finally, the pose estimation was based on normal musculoskeletal alignment. Conditions different from normal alignment such as using large assist devices, prosthesis, or large bone deformity that makes a misestimation of keypoints might affect the accuracy. Despite these limitations, the single camera-based pose estimation using OP is acceptable for measuring temporo-spatial parameters and some hip and knee joint kinematics parameters.

V. Conclusion

The present study aimed to investigate the capability of a single RGB camera-based pose estimation system to measure temporo-spatial and sagittal plane joint kinematics during gait with orthosis. The results indicated that this system using OP can measure the several temporo-spatial parameters with high agreement and consistency under various gait conditions. Although the ankle kinematics parameter did not reveal measurement reliability compared to 3DMC, this system could acceptably measure the hip and knee kinematics information during gait from the results. Further study is to investigate pathological participants, and evaluate the lower extremity of other plane kinematics for use in clinical sites.

References

[1] S. Porta, A. Martínez, N. Millor, M. Gómez, and M. Izquierdo, "Relevance of sex, age and gait kinematics when predicting fall-risk and mortality in older adults," *J. Biomech.*, vol. 105, May 2020, Art. no. 109723, doi: 10.1016/j.jbiomech.2020.109723.

[2] J. S. Sulzer, K. E. Gordon, Y. Y. Dhaher, M. A. Peshkin, and J. L. Patton, "Preswing knee flexion assistance is coupled with hip abduction in people with stiff-knee gait after stroke," *Stroke*, vol. 41, no. 8, pp. 1709–1714, Aug. 2010, doi: 10.1161/STROKEAHA.110.586917.

[3] L. N. Awad *et al.*, "A soft robotic exosuit improves walking in patients after stroke," *Sci. Transl. Med.*, vol. 9, no. 400, pp. 1–13, Jul. 2017, doi: 10.1126/scitranslmed.aai9084.

[4] A. H. Mackey, S. E. Walt, G. A. Lobb, and N. S. Stott, "Reliability of upper and lower limb three-dimensional kinematics in children with hemiplegia," *Gait Posture*, vol. 22, no. 1, pp. 1–9, Aug. 2005, doi: 10.1016/j.gaitpost.2004.06.002.

[5] G. Yavuzer, Ö. Öken, A. Elhan, and H. J. Stam, "Repeatability of lower limb three-dimensional kinematics in patients with stroke," *Gait Posture*, vol. 27, no. 1, pp. 31–35, Jan. 2008, doi: 10.1016/j.gaitpost.2006.12.016.

[6] G. Paolini *et al.*, "Validation of a method for real time foot position and orientation tracking with Microsoft Kinect technology for use in virtual reality and treadmill based gait training programs," *IEEE Trans. Neural Syst. Rehabil. Eng.*, vol. 22, no. 5, pp. 997–1002, Sep. 2014, doi: 10.1109/TNSRE.2013.2282868.

[7] S. Springer and G. Y. Seligmann, "Validity of the Kinect for gait assessment: A focused review," *Sensors*, vol. 16, no. 2, p. 194, 2016, doi: 10.3390/s16020194.

[8] R. A. Clark, K. J. Bower, B. F. Mentiplay, K. Paterson, and Y.-H. Pua, "Concurrent validity of the Microsoft Kinect for assessment of spatiotemporal gait variables," *J. Biomech.*, vol. 46, no. 15, pp. 2722–2725, Aug. 2013, doi: 10.1016/j.jbiomech.2013.08.011.

[9] B. F. Mentiplay *et al.*, "Gait assessment using the Microsoft Xbox One Kinect: Concurrent validity and inter-day reliability of spatiotemporal and kinematic variables," *J. Biomech.*, vol. 48, no. 10, pp. 2166–2170, Jul. 2015, doi: 10.1016/j.jbiomech.2015.05.021.

[10] Y.-Y. Liao, I.-H. Chen, and R.-Y. Wang, "Effects of Kinect-based exergaming on frailty status and physical performance in prefrail and frail elderly: A randomized controlled trial," *Sci. Rep.*, vol. 9, no. 1, pp. 1–9, Dec. 2019, doi: 10.1038/s41598-019-45767-y.

[11] T. Matsuura, K. Sakashita, A. Grushnikov, F. Okura, I. Mitsugami, and Y. Yagi, "Statistical analysis of dual-task gait characteristics for cognitive score estimation," *Sci. Rep.*, vol. 9, no. 1, pp. 1–12, Dec. 2019, doi: 10.1038/s41598-019-56485-w.

[12] A. Kendall, M. Grimes, and R. Cipolla, "PoseNet: A convolutional network for real-time 6-DOF camera relocalization," in *Proc. IEEE Int. Conf. Comput. Vis. (ICCV)*, Dec. 2015, pp. 2938–2946, doi: 10.1109/ICCV.2015.336.

[13] Z. Cao, T. Simon, S.-E. Wei, and Y. Sheikh, "Realtime multi-person 2D pose estimation using—Part affinity fields," in *Proc. IEEE Conf. Comput. Vis. Pattern Recognit. (CVPR)*, Jul. 2017, pp. 1302–1310, doi: 10.1109/CVPR.2017.143.

[14] R. Guo, X. Shao, C. Zhang, and X. Qian, "Sparse adaptive graph convolutional network for leg agility assessment in Parkinson's disease," *IEEE Trans. Neural Syst. Rehabil. Eng.*, vol. 28, no. 12, pp. 2837–2848, Dec. 2020, doi: 10.1109/TNSRE.2020.3039297.

[15] E. D'Antonio, J. Taborri, E. Palermo, S. Rossi, and F. Patane, "A markerless system for gait analysis based on OpenPose library," in *Proc. IEEE Int. Instrum. Meas. Technol. Conf. (I2MTC)*, May 2020, pp. 1–6, doi: 10.1109/I2MTC43012.2020.9128918.

[16] S. Hesse, C. Werner, K. Matthias, K. Stephen, and M. Berteanu, "Non–velocity-related effects of a rigid double-stopped ankle-foot orthosis on gait and lower limb muscle activity of hemiparetic subjects with an equinovarus deformity," *Stroke*, vol. 30, no. 9, pp. 1855–1861, Sep. 1999, doi: 10.1161/01.STR.30.9.1855.

[17] S. Tyson, E. Sadeghi-Demneh, and C. Nester, "A systematic review and meta-analysis of the effect of an ankle-foot orthosis on gait biomechanics after stroke," *Clin. Rehabil.*, vol. 27, no. 10, pp. 879–891, Oct. 2013, doi: 10.1177/0269215513486497.

[18] T. Kobayashi, M. S. Orendurff, M. L. Singer, F. Gao, W. K. Daly, and K. B. Foreman, "Reduction of genu recurvatum through adjustment of plantarflexion resistance of an articulated ankle-foot orthosis in individuals post-stroke," *Clin. Biomech.*, vol. 35, pp. 81–85, Jun. 2016, doi: 10.1016/j.clinbiomech.2016.04.011.

[19] J. Perry, M. Garrett, J. K. Gronley, and S. J. Mulroy, "Classification of walking handicap in the stroke population," *Stroke*, vol. 26, no. 6, pp. 982–989, Jun. 1995, doi: 10.1161/01.STR.26.6.982.

[20] A. Schmid *et al.*, "Improvements in speed-based gait classifications are meaningful," *Stroke*, vol. 38, no. 7, pp. 2096–2100, Jul. 2007, doi: 10.1161/STROKEAHA.106.475921.

[21] F. Yang and G. A. King, "Dynamic gait stability of treadmill versus overground walking in young adults," *J. Electromyogr. Kinesiol.*, vol. 31, pp. 81–87, Dec. 2016, doi: 10.1016/j.jelekin.2016.09.004.

[22] M. Andrews, F. R. Noyes, T. E. Hewett, and T. P. Andriacchi, "Lower limb alignment and foot angle are related to stance phase knee adduction in normal subjects: A critical analysis of the reliability of gait analysis data," *J. Orthopaedic Res.*, vol. 14, no. 2, pp. 289–295, Mar. 1996.

[23] M. A. Hunt *et al.*, "Lateral trunk lean explains variation in dynamic knee joint load in patients with medial compartment knee osteoarthritis," *Osteoarthritis Cartilage*, vol. 16, no. 5, pp. 591–599, May 2008, doi: 10.1016/j.joca.2007.10.017.

[24] G. Francini *et al.*, "Gait & posture reliability and minimum detectable change of the gait pro file score for post-stroke patients," *Gait Posture*, vol. 49, pp. 382–387, Sep. 2016, doi: 10.1016/j.gaitpost.2016.07.149.

[25] J. A. Zeni, J. G. Richards, and J. S. Higginson, "Two simple methods for determining gait events during treadmill and overground walking using kinematic data," *Gait Posture*, vol. 27, no. 4, pp. 710–714, 2008, doi: 10.1016/j.gaitpost.2007.07.007.

[26] T. Kobayashi, M. L. Singer, M. S. Orendurff, F. Gao, W. K. Daly, and K. B. Foreman, "The effect of changing plantarflexion resistive moment of an articulated ankle–foot orthosis on ankle and knee joint angles and moments while walking in patients post stroke," *Clin. Biomech.*, vol. 30, no. 8, pp. 775–780, Oct. 2015, doi: 10.1016/j.clinbiomech.2015.06.014.

[27] H. Hsiao, B. A. Knarr, J. S. Higginson, and S. A. Binder-Macleod, "Mechanisms to increase propulsive force for individuals poststroke," *J. NeuroEng. Rehabil.*, vol. 12, no. 1, pp. 1–8, Dec. 2015, doi: 10.1186/s12984-015-0030-8.

[28] Y. Sekiguchi *et al.*, "Ankle–foot orthosis with dorsiflexion resistance using spring-cam mechanism increases knee flexion in the swing phase during walking in stroke patients with hemiplegia," *Gait Posture*, vol. 81, pp. 27–32, Sep. 2020, doi: 10.1016/j.gaitpost.2020.06.029.

[29] C. M. Tyrell, M. A. Roos, K. S. Rudolph, and D. S. Reisman, "Influence of systematic increases in treadmill walking speed on gait kinematics after stroke," *Phys. Therapy*, vol. 91, no. 3, pp. 392–403, Mar. 2011, doi: 10.2522/ptj.20090425.

[30] H. Hsiao, B. Knarr, J. Higginson, and S. Binder-Macleod, "The relative contribution of ankle moment and trailing limb angle to propulsive force during gait," *Hum. Movement Sci.*, vol. 39, pp. 212–221, Oct. 2015, doi: 10.1016/j.humov.2014.11.008.

[31] J. M. Bland and D. G. Altman, "Statistical methods for assessing agreement between two methods of clinical measurement," *Lancet*, vol. 327, no. 8476, pp. 307–310, Feb. 1986.

[32] D. V. Cicchetti, "Guidelines, criteria, and rules of thumb for evaluating normed and standardized assessment instruments in psychology," *Psychol. Assessment*, vol. 6, no. 4, pp. 284–290, 1994.

[33] M. B. Pohl, N. Messenger, and J. G. Buckley, "Forefoot, rearfoot and shank coupling: Effect of variations in speed and mode of gait," *Gait Posture*, vol. 25, no. 2, pp. 295–302, Feb. 2007, doi: 10.1016/j.gaitpost.2006.04.012.

[34] E. Dolatabadi, B. Taati, and A. Mihailidis, "Concurrent validity of the Microsoft Kinect for Windows v2 for measuring spatiotemporal gait parameters," *Med. Eng. Phys.*, vol. 38, no. 9, pp. 952–958, Sep. 2016, doi: 10.1016/j.medengphy.2016.06.015.

[35] A. M. Barthuly, R. W. Bohannon, and W. Gorack, "Gait speed is a responsive measure of physical performance for patients undergoing short-term rehabilitation," *Gait Posture*, vol. 36, no. 1, pp. 61–64, 2012, doi: 10.1016/j.gaitpost.2012.01.002.

[36] C. Schiefer *et al.*, "Optimization of inertial sensor-based motion capturing for magnetically distorted field applications," *J. Biomech. Eng.*, vol. 136, no. 12, pp. 1–8, Dec. 2014, doi: 10.1115/1.4028822.

[37] X. Robert-Lachaine, H. Mecheri, C. Larue, and A. Plamondon, "Validation of inertial measurement units with an optoelectronic system for whole-body motion analysis," *Med. Biol. Eng. Comput.*, vol. 55, no. 4, pp. 609–619, Apr. 2017, doi: 10.1007/s11517-016-1537-2.

[38] M. Al-Amri, K. Nicholas, K. Button, V. Sparkes, L. Sheeran, and J. L. Davies, "Inertial measurement units for clinical movement analysis: Reliability and concurrent validity," *Sensors*, vol. 18, no. 3, pp. 1–29, 2018, doi: 10.3390/s18030719.

[39] X. Xu, R. W. McGorry, L.-S. Chou, J.-H. Lin, and C.-C. Chang, "Accuracy of the Microsoft Kinect for measuring gait parameters during treadmill walking," *Gait Posture*, vol. 42, no. 2, pp. 145–151, Jul. 2015, doi: 10.1016/j.gaitpost.2015.05.002.

[40] M. D. Lewek and G. S. Sawicki, "Trailing limb angle is a surrogate for propulsive limb forces during walking post-stroke," *Clin. Biomech.*, vol. 67, pp. 115–118, Jul. 2019, doi: 10.1016/j.clinbiomech.2019.05.011.

[41] A. Pfister, A. M. West, S. Bronner, and J. A. Noah, "Comparative abilities of Microsoft Kinect and Vicon 3D motion capture for gait analysis," *J. Med. Eng. Technol.*, vol. 38, no. 5, pp. 274–280, 2014, doi: 10.3109/03091902.2014.909540.

[42] M. Eltoukhy, J. Oh, C. Kuenze, and J. Signorile, "Improved Kinect-based spatiotemporal and kinematic treadmill gait assessment," *Gait Posture*, vol. 51, pp. 77–83, Jan. 2017, doi: 10.1016/j.gaitpost.2016.10.001.

[43] B. F. Mentiplay, M. Banky, R. A. Clark, M. B. Kahn, and G. Williams, "Lower limb angular velocity during walking at various speeds," *Gait Posture*, vol. 65, pp. 190–196, Sep. 2018, doi: 10.1016/j.gaitpost.2018.06.162.